Estimating daily passive fish abundance in an open estuary from sparse data in spatio-temporal sampling: particular case of glass eel flows

Noëlle Bru, Michel Lejeune, Patrick Prouzet

Estimating daily passive fish abundance in an open estuary from sparse data in spatio-temporal sampling :

particular case of glass eel flows.

Noëlle Bru[(1)], Michel Lejeune[(2)], Patrick Prouzet[(3)]

[(1)] Laboratoire de Mathématiques Appliquées (CNRS UMR 5142) / IUT STID

Université de Pau et des Pays de l'Adour, BP1155

64013 Pau Cedex, France

Tel. : (33) 05 59 40 71 43   Fax. : (33) 05 59 40 71 25

e-mail : noelle.bru@univ-pau.fr

[(2)] Laboratoire de Statistique et d'Analyse des Données, Université Pierre Mendès-France,

Bâtiment Sciences de l'Homme et des Mathématiques, BP 47,

38040 Grenoble Cedex 9, France

[(3)] Laboratoire Halieutique d'Aquitaine IFREMER

Maison du Parc, Technopole Izarbel Côte Basque,

64210 Bidart, France

Abstract

A methodology to estimate glass eel (*Anguilla anguilla* L.) abundance on a daily basis containing sparse data is proposed.

Our analyses are based on scientific *in situ* campaigns data coming from a sampling protocol which leads to spatio-temporal blanks in the fish distribution along the estuary and the time period that must be taken into account in fish abundance estimate calculated using the sparse data.

Estimates at each catch locations are calculated and then extended to the whole section of the river from a Bayesian extrapolation approach which leads to a spatially explicit method.

The method proposed a resulting estimator assessing a non-linear model of current speed (a crucial element for the behaviour of this passive fish) and the sampling design jointly being able to estimate the abundance of glass eel migrating during a given day in the presence of sparse data.

Confidence intervals are also proposed calculated using the sensitivity of the biomass estimates to the statistical methodology and the choice of spatial extrapolation.

2

1. INTRODUCTION

European Eel (*Anguilla anguilla* L.) is a valuable resource from an economical point of view for small scale fisheries in Europe (Léauté *et al.* 2002, Prouzet *et al.* 2002).

This fish resource is considered in danger by the ICES (Anonymous 2003) and consequently the Commission of the European Community made a proposal for establishing reliable measures of the stock of European Eel (Anonymous 2003). A constant decrease of the glass eel catches has been observed since the seventies in the Bay of Biscay and earlier in the scandinavian areas. Several suggestions for possible causes of decline of the number of glass eel entering rivers have include over-exploitation at the different phases of the biological cycle, inland habitat loss, climate and ocean current change, disease, degradation of continental environment and pollution, with no single obvious cause (Prouzet 2003). An estimate of biomass is needed in order to calculate the rate of exploitation thanks to the knowledge of the eel catches and so to assess the fishing impact of the glass eel in estuaries. The present study constitutes a first step in the implementation of mechanisms which will allow to achieve this objective.

The estimation of fish abundance is a classical problem in fishery science of key importance to manage any fishery resources. One problem is to obtain a reliable estimate of fish abundance. The absolute fish abundance in an open area is hard to obtain. Most methods are designed for a fixed stock within a given area of a stream or a lake. A classical approach, for instance, is that of Hankin and Reeves (1988) dealing with visual counts, while recently Rivoirard *et al.* (2000) proposed the use of a geostatistical approach. An extensive review can be found in Schwarz and Seber (1999). Hydroacoustics campaigns also give significant results for dense aggregation structure of fish and capture-mark-recapture methods too but are not easily implemented with glass eel. From now on, for the glass eel problem, the most part of biomass estimates come from fishing data but this is a very crude measure with possible bias due to a variation of fish

catchability which is used rather as a qualitative or relative indicator of stock size rather than a quantitative and absolute one. So, scientific research trawl surveys were conducted to define an objective abundance index and to obtain more accurate estimates for an entire area. Recently, Chen *et al.* (2004) proposed a fish abundance indices also based on scientific research trawl surveys via a model-based prediction approach using loglinear regression and nonparametric smoothing. Two sources of variation are taken into account in their work : the variation due to the catching process (estimation stage) and the variation due to the sampling design stage. This point of view is also our point of view but the peculiarity of our work is due to the sparsity of the data sets which restrains the use of Chen *et al.*'s method.

The objective of this work is to built a framework where two sources of randomness are entertained which are : the behaviour of the glass eel and the sampling protocol. Our method proposed a resulting estimator assessing a model of current speed and the sampling design jointly being able to estimate the abundance of glass eel migrating during a given day in the presence of sparse data. Confidence intervals are also proposed calculated using the sensitivity of our biomass estimates to our statistical methodology and to the choice of spatial extrapolation.

2. SOME PRECISIONS ON THE DATA AND FIRST FORMULA TO COMPUTE BIOMASS

2.1 The glass eel ecological background.

The Leptocephalae arrive on the european continental shelf around the end of the summer and metamorphosed in glass eel. During its migration from the continental shelf to the river, the glass eel has to move through the estuary. For a given river, the most important period of migration can vary according to the latitude and the geographical area (Mediterranean Sea and Atlantic coast).

The size of the glass eel is ranged between 6 and 8cm and the weight is around 0.3g. The musculature of the glass eel is weakly developed and the swim-bladder is not operative (no gas

inside). These physiological characteristics restrict, of course, the swimming performance of glass eel when they migrate through the estuary (Cantrelle 1981). On the basis of previous knowledge (Désaunay *et al.* 1993) it seems that glass eel tend to move upstream more intensively the faster the flood tide speed is. Moreover, some observations on the Adour river showed that the migration is mainly a drift with the tide current, the glass eel staying behind the dynamic front of the tide (Prouzet *et al.* 2003). This is somewhat explained by the fact that their effort is then minimized. For that reason the most part of their migration is passive along the fluvial axis (using the flood tide defined as the current which runs from the sea inside the river) in a complex environment where the salt and freshwater meet. The propagation of the dynamic tide was observed to control the upstream migration of the glass eel towards the freshwater zone and that glass eel cannot swim against a current the speed of which is greater than 20cm per second and do not seem present in the water column when the speed is higher (Prouzet 2003).

During flood tide, glass eel migrate vertically in the water column using active vertical movements, with a dispersion of the individuals on the banks surface and in the medium part of the estuary. The glass eel can go up on the surface to use more favourable currents to continue their upstream migration. During the ebb-tide when the current is directed against the glass eel, they generally stop their migration and hide in the ground. The glass eel concentration available into the estuary would be then a function of the intensity of the currents.

2.2 Physical setting, sampling protocol and data.

Our approach takes the temporal distribution pattern of the glass eel flows densities during the flood tide and the spatial behaviour of glass eel into the water column into account. To achieve this, a sampling protocol considering space and time variability of the glass eel migratory behaviour was constructed using survey techniques.

The data arise from catches made by night, approximately from the beginning until the end of the flood tide (almost 6 hours) corresponding to the main part of the glass eel daily migratory period. Samples were taken successively on three transects: one near the right bank (RB), the other one in the middle of the river (M) and the last one near the left bank (LB).

Each sample results from catches by means of small nets hauled from a boat moving down the river (*i.e.* opposite to the stream current direction) during five minutes. Two catches were made simultaneously: on the surface (1m deep) and at a depth about four meters, with a comparable fishing gear (see Figure 1).

(insert Figure 1)

A complete sampling cycle took about 30 minutes, which allowed (at the most) only eight cycles (mainly between 5 and 8) per night. For each samples (around 48), glass eel are weighted and a density of glass eel (in $g.(100m^3)^{-1}$) could then be calculated considering the volume of water filtered, depending on the relative speed of the boat. The sampling protocol is detailed in Prouzet *et al.* (2003).

2.3 Construction of an estimator of the daily glass eel biomass

Let denote by R the vertical region of the river also called "total water column" or "section" (in m^2) which corresponds to a average design during the sampling period (for simplification we did not consider the variation of the water level during the period and used an average value). For a given day, we are interested in the evaluation of the total biomass $B(R)$, named the daily glass eel biomass (in g or kg), which has come trough R during the flood tide period $[t_1, t_2]$. This quantity can be computed by:

$$B(R) = \sum_{s \in R} \left(\int_{t_1}^{t_2} d_s(t) v_s(t) dt \right) surface(R), \qquad \text{(Eq. 1)}$$

7

using the current speed $v_s(t)$ in m.s^{-1} and the glass eel densities $d_s(t)$ in g.(100m^3)$^{-1}$ which is the glass eel information we only have.

3. MODELIZATION ASPECTS.

One difficulty is that formula (Eq. 1) makes appear the need of having a functional form for the glass eel density and the current speed.

3.1 Modelling the spatio-temporal evolution of the current speed

The aim of this section is to develop a model for the river current at the section where the sampling occurred based on the *in situ* values of current speed. This model will be useful to compute *B(R)* in two ways: one is to give a functional evolution of the current speed during the flood tide and the other is to determinate as precisely as possible the beginning and the end of the flood tide (labelled as a positive current in the following) at the considered section corresponding to the period of the rising tide. The model was established under the following hypotheses:

(i)   for a given transect, the current speed is the same within the whole water column;

(ii)   for any transect, the current depends on time by a sinusoïdal form. Only the positive part of this relation corresponding to the flood tide is used in this study;

(iii)   At each point (RB, M and LB), the positive current starts and ends at the same time. Only its intensity may differ.

Let t_{ik} be the time point where speed is measured for transect i (with i=1, 2, 3 coding for RB, M and LB) and passing cycle k (with k=1,…, n and n generally equal to 8) during the given day. Thus, the observed current speed v_i for transect i at time point t_{ik} is assumed to follow:

$$v_i(t_{ik}) = c_i \sin\left[\frac{\pi}{a}(t_{ik} - b)\right] + \varepsilon_{ik}^{(1)}. \qquad \text{(Eq. 2)}$$

8

The parameters of this model are:

- a, the duration of the flood tide (in min),

- c_i, the maximal intensity (in m.s^{-1}) of the current speed on transect i,

- b, the time (in min) of the beginning of the flood tide relatively to the beginning of the sampling protocol ($t=0$). Usually b is negative, *i.e.* the latter started after the flood tide had begun (also it usually ended before the end of it).

- the variance of the error terms $\varepsilon_{ik}^{(1)}$ is supposed to be constant. Moreover these terms are assumed to have zero mean (unbiased measure of current speed) and to be uncorrelated.

These parameters, as well as the associated standard errors for a, b and the c_i's, are estimated by a classical iterative procedure for non linear regression using Splus software.

We can then write : $t_1 = b$ and $t_2 = a + b$ and we can easier discuss on the sampling protocol using a et b.

3.2 Modelling glass eel densities as a function of current speed

The only clear element of knowledge about glass eel behaviour is that they need the flood tide to come in, in order to move up the river. As for the distribution in space, it must be assumed that the fishes may migrate upwards anywhere in that section. This model will serve the extrapolation of the glass eel flow in time, at a given space point, during the flood tide.

Let P be the weight (in g) of fish collected at some point in time and in space. This weight corresponds to a catch through a fixed section 0.33m^2 of the trawled net and during a fixed time Δt of five minutes (*i.e.* 300s). The resulting density (in g.(100m^3)$^{-1}$) is:

$$d = \frac{\text{weigth of collected glass eel}}{\text{volume of filtered water}} = \frac{100 \times P}{v \times 0{,}33 \times \Delta t}, \qquad \text{(Eq. 3)}$$

where v is the observed relative speed of the boat (in m.s^{-1}).

In view of the weak number of available data, an error of measure on glass eel densities turns out catastrophic for a statistical model. Therefore, we are going to correct the possible errors by means of the current speed model (Eq. 2) which allows to estimate the relative speed of the boat which enters the computation of density for a given catch. So, from now on , v is replaced by the speed of the current now as estimated model (Eq. 2), plus boat speed relative to the bottom (exact measure).

Thus, on the basis of previous knowledge, it seemed natural to use stream speed as an explanatory variable for density. To eliminate clear problems of heteroscedasticity a log-transformation was operated on both variables, leading to the following linear model:

$$\log d_{sk} = \alpha_s \log v_{sk} + \beta_s + \varepsilon_{sk}^{(2)}, \qquad\qquad (\text{Eq. 4})$$

where s indicates one of the six locations of measurement and k is the cycle through the three transects during the given day ($k=1,\ldots,, n$). A different model is fitted at each location since there is no reason to believe that density is homogeneous in the transects from RB to LB and from surface to bottom. Note that, assuming $s=1, 2, 3$ at the surface and $s=4, 5, 6$ at the bottom, hypothesis (i) on current speed (see previous section) implies that $v_{sk} = v_{s+3,k}$.

However, because we have few points available at each location (at most $n=8$) we will pool estimated variance terms together to get a single variance estimate based on a larger number of observations. Doing so we assume that the error terms $\varepsilon_{sk}^{(2)}$ are uncorrelated and have constant variance in time and space. We will see in next section that single estimates remain rather similar, which justifies the hypothesis of a constant variance. The lack of correlation did not seem too critical either. As a matter of fact, empirical autocorrelation between measurements was found to be negligible since density is highly variable in time and the time span from one location to the

next one was relatively high (about 10min). Moreover, there was even no significant correlation between the top and the bottom measurements taken at the same time.

4. BIOMASS ESTIMATE : COMPUTATION AND PROPERTIES.

Let denote by $\hat{d}_s(t)$ and $\hat{v}_s(t)$ the estimation of $d(t)$ et $v(t)$ on every time points obtained by (Eq. 4) and (Eq. 2).

The second difficulty of computing (Eq. 1) is we only have observation data of $d_s(t)$ on 6 points. So, the remaining problem is how to extrapolate the expected biomass at the six sampling locations to the entire section of the river. Needless to say that we have too little information and too little *a priori* knowledge to be able to build a spatial model at time *t*. Moreover, we never observed the six locations at the same time but during a time span of about 30 minutes corresponding to a complete sampling cycle. Thus, considering the high variability of the catches in time, it is not sensible to consider the catches as simultaneous at these different locations. Consequently, we used an empirical approach at the aggregate level of the biomass estimated at each location as above, *i.e.* for the whole day period. So, we split the region *R* into a grid compounded by *S* rectangle cells, each containing a sampling point *s* (so *S=6* in our example). As the choice of the sampled grid can induce a source of non negligible randomness, we test *J* different selections (or schemes) of sampling units grid. A given scheme is thus corresponding to an implicit gradient of extrapolation in the two dimensions *i.e.* width and depth. Since it would have been too penalizing to use the most extreme schemes as a term of uncertainty, we favoured a Bayesian approach giving equal probability to each of them. Each part *s* of the grid rectangle associated to one cut out *j* of the region *R* has a surface (in m²) denoted by S_{sj}, *s=1,...,S* and

11

j=1,...,J. This discretization is equivalent to assuming that the biomass is constant within each grid rectangle.

With this convention, our practical definition of the glass eel biomass estimate is as follows :

$$\hat{B}(R) = \frac{1}{J} \sum_{j=1}^{J} \sum_{s=1}^{S} \left(\int_{t_1}^{t_2} \hat{d}_s(t) \hat{v}_s(t) dt \right) S_{sj}, ,$$

(Eq. 5)

Above formula takes into account some characteristics of the stream with $\hat{v}_s$ and of the two dimensional spatial structure S_{sj} in which the sample unit *s* is selected according to the same principle as Overton *et al.* (1998).

To elaborate a method of estimation of the daily biomass including a term of uncertainty, the main sources of error have to be first identified in (Eq. 5). As far as the density measures are concerned, it is assumed that errors on the weight of the catch as well as on the section of the trawled net are negligible. However the value of the boat speed relative to the surface is quite approximate, while the speed relative to the bottom is precise, both used in the computation of the current speed. The greatest difficulty and, at the same time the largest source of error, stems from the extrapolation of a few discrete measurements to a process which is continuous in time and in space. The exact speed at time *t* is $c_s \sin\left[\frac{\pi}{a}(t-b) \right]$, and can be estimated from model (Eq. 2) by

$\hat{v}_s(t) = \hat{c}_s \sin\left[\frac{\pi}{\hat{a}}\left(t - \hat{b}\right) \right]$. Model (Eq. 4) yields an estimator of $d_s(t)$ of the form

$\hat{d}_s(t) = \exp(\hat{\beta}_s)[v_s(t)]^{\hat{\alpha}_s}$. In this expression, $v_s(t)$ is unknown and can only be estimated by $\hat{v}_s(t)$. However, we will neglect this source of error which can be considered as being of second order with respect to errors on $\hat{\beta}_s$ and $\hat{\alpha}_s$. So,

$$\int_{\hat{b}}^{\hat{a}+\hat{b}} \hat{d}_s(t) \hat{v}_s(t) dt = \exp(\hat{\beta}_s) \int_{\hat{b}}^{\hat{a}+\hat{b}} [\hat{v}_s(t)]^{\hat{\alpha}_s+1} dt = \frac{1}{\pi} \exp(\hat{\beta}_s) \hat{c}_s^{\hat{\alpha}_s+1} \hat{a} \int_0^\pi \sin^{\hat{\alpha}_s+1}(u) du ,$$

and,

$$\hat{B}(R) = \frac{1}{J} \sum_{j=1}^{J} \sum_{s=1}^{S} \left(\frac{1}{\pi} \exp(\hat{\beta}_s) \hat{c}_s^{\hat{\alpha}_s+1} \hat{a} \int_0^{\pi} \sin^{\hat{\alpha}_s+1}(u) du \right) S_{sj}.$$

We need now to determine the expectation of $\hat{B}(R)$ as well as its variance since we aim at a confidence interval on our daily estimate $\hat{B}(R)$. Let denote by

$$\hat{B}_s = \frac{1}{\pi} \exp(\hat{\beta}_s) \hat{c}_s^{\hat{\alpha}_s+1} \hat{a} \int_0^{\pi} \sin^{\hat{\alpha}_s+1}(u) du, \; s=1,...,6, \text{ and } \hat{B}_j = \sum_{s=1}^{S} \hat{B}_s S_{sj} \text{ and finally, } \hat{B}(R) = \frac{1}{J} \sum_{j=1}^{J} \hat{B}_j.$$

Since exact expressions are not attainable, we will use the following general approximations: consider $I = g(X_1,...,X_p,t)$ where $X_1,...,X_p$ are random variables, then, with obvious notations,

$$E(I) \approx g(E(X_1),...,E(X_p),t) \text{ and } V(I) \approx \sum_{i=1}^{p} V(X_i) \left[\frac{\partial}{\partial x_i} g(E(X_1),...,E(X_p),t) \right]^2$$

$$+ 2 \sum_{i<j} \text{cov}(X_i X_j) \left[\frac{\partial}{\partial x_i} g(E(X_1),...,E(X_p),t) \times \frac{\partial}{\partial x_j} g(E(X_1),...,E(X_p),t) \right]$$

(This can be easily established by using a Taylor expansion of g around $(E(X_1),...,E(X_p))$, at order one for the expectation and order two for the variance).

To simplify the writings let us drop, for the time being, the location index s of $\hat{B}_s$. Consequently, $\hat{B}$ is approximately unbiased and its variance can be approximated by:

$$V(\hat{B}) \approx V(\hat{\beta})I_1^2 + V(\hat{c})I_2^2 + V(\hat{a})I_3^2 + V(\hat{\alpha})I_4^2 + 2\text{cov}(\hat{a},\hat{\beta})I_1 I_4 + 2\text{cov}(\hat{a},\hat{c})I_2 I_3, \quad \text{(Eq. 6)}$$

where:

$$I_1 = \frac{1}{\pi} \exp(\hat{\beta}) \hat{c}^{\hat{\alpha}+1} \hat{a} \int_0^{\pi} \sin^{\hat{\alpha}+1}(u) du = \hat{B}, \quad \text{(Eq. 7)}$$

$$I_2 = \frac{\hat{\alpha}+1}{\pi} \exp(\hat{\beta}) \hat{c}^{\hat{\alpha}} \hat{a} \int_0^{\pi} \sin^{\hat{\alpha}+1}(u) du = \frac{\hat{\alpha}+1}{\hat{c}} \hat{B}, \quad \text{(Eq. 8)}$$

$$I_3 = \frac{1}{\pi} \exp(\hat{\beta}) \hat{c}^{\hat{\alpha}+1} \int_0^\pi \sin^{\hat{\alpha}+1}(u) du = \frac{1}{\hat{a}} \hat{B},$$
(Eq. 9)

$$I_4 = \hat{B} \log \hat{c} + \frac{1}{\pi} \exp(\hat{\beta}) \hat{c}^{\hat{\alpha}+1} \hat{a} \int_0^\pi \log(\sin u). \sin^{\hat{\alpha}+1}(u) du.$$
(Eq. 10)

Note that the covariances between estimators coming from a different model have been neglected in this estimated variance.

While fitting models (Eq. 2) and (Eq. 4), one obtains estimates of the variances and covariances in equation (Eq. 6). Thus $\hat{B}_s$ and the estimate $s^2(\hat{B}_s)$ of $V(\hat{B}_s)$ can be numerically computed.

Since $\int_0^\pi \sin^{\hat{\alpha}+1}(u) du = 2 \int_0^{\pi/2} (\sin u)^{2\left(\frac{\hat{\alpha}+2}{2}\right)-1} du = B\left(\frac{1}{2}, \frac{\hat{\alpha}+2}{2}\right) = \frac{\sqrt{\pi} \Gamma\left(\frac{\hat{\alpha}+2}{2}\right)}{\Gamma\left(\frac{\hat{\alpha}+3}{2}\right)},$ where $B(.,.)$ and

$\Gamma(.,.)$ are respectively the beta and the gamma functions, only I_4 requires a specific numerical integration (the Splus software was used for this purpose).

For scheme j, we may then write the estimated variance of $\hat{B}_j = \sum_{s=1}^{S} \hat{B}_s S_{sj}$:

$$s^2(\hat{B}_j) = \sum_{s=1}^{S} s^2(\hat{B}_s) S_{sj}^2,$$
(Eq. 11)

assuming no correlation between the estimates at different locations.

Then the final point estimate is just $\hat{B}(R) = \frac{1}{J} \sum_{j=1}^{J} \hat{B}_j$ and, using a two variance components formula, the variance estimate is:

$$s^2(\hat{B}(R)) = \frac{1}{J} \sum_{j=1}^{J} s^2(\hat{B}_j) + \frac{1}{J} \sum_{j=1}^{J} (\hat{B}_j - \hat{B}(R))^2.$$
(Eq. 12)

An approximate 95% confidence interval for the daily glass eel total biomass $B(R)$ is thus given by: $IC_{95\%}(B(R)) \approx [\hat{B}(R) - 2s(\hat{B}(R)); \hat{B}(R) + 2s(\hat{B}(R))].$

5. NUMERICAL RESULTS

This methodology is first applied to data collected into the Adour estuary by IFREMER
(Laboratoire Ressources Halieutiques d'Aquitaine). The Adour estuary is situated in South-West
France (43°30'N and 1°32'W). The section where the experimental catches took place is located
15km away from the mouth of the river (Figure 2).

(Insert Figure 2)

Several seasons of glass eel migration (each from November till March) were studied since 1998.
To illustrate the above methodology we present the detailed results of a specific day, the 9th
December 1999, which was found to be the most important day of migration of the corresponding
fishing season and so gives a good idea of the highest level of glass eel biomass.

On that day, there were 8 cycles, *i.e.* a total of 24 measurements of current speed and 48
measurements of glass eel density.

5.1 Modelling data for the 9th December 1999

Using the sinusoidal model (eq. 2), one obtains r^2=0.88 (based on 24 data points) and the
parameters estimates with their standard errors in Table 1.

(Insert Table 1)

The estimated covariances between the parameters may be derived from the correlation matrix.

Figure 3 plots the predicted and observed current speeds, and illustrates the errors of
measurement and the fact that the sampling protocol had started after the flood tide had begun
(first measurement up to the horizontal axis at 0).

(Insert Figure 3)

Figure 4 plots glass eel density (in g.(100m^3)$^{-1}$) as calculated by formula (Eq. 3) versus
(modelized) current speed and shows a clear problem of heteroscedasticity.

15

(Insert Figure 4)

Using the log-log model for, say, the bottom and middle location ($s=5$, see Figure 5) with 8 data points, one obtains $r^2=0.22$. The estimates of parameters α_5 and β_5 as well as their standard errors are in Table 2.

(Insert Table 2)

(Insert Figure 5)

The estimated asymptotic correlation for the two estimates is equal to 0.71. The previous parameter estimates are used to compute $\hat{B}_5$ and I_1, I_2, I_3 and I_4 in (Eq. 6). Thus, using $\int_0^\pi \sin^{\hat{\alpha}+1}(u)du = 1.82$ and $\int_0^\pi \log(\sin u)\sin^{\hat{\alpha}+1}(u)du = -0.5$, one obtains $\hat{B}_5 = 1.7\,kg$ for the bottom-middle location (see Table 3).

(Insert Table 3)

5.2 Estimation of glass eel biomass : 9th December 1999.

The estimation for the 9 December 1999 was finally obtained by spatial extrapolation based on a set of 12 splitting schemes of the whole section. These were ranging from a narrow width to a large one on the edges, and from a shallow one to a deeper one to separate the high and the low locations (see Table 4).

(Insert Table 4)

From formula (Eq. 11), one derives the estimated biomass $\hat{B}_3$ corresponding to this scheme and its standard error:

$$\begin{cases} \hat{B}_3 = 1474\,kg, \\ s(\hat{B}_3) = 304\,kg. \end{cases}$$

The corresponding estimated biomasses (in kg) for the 12 spatial schemes are given in Table 5.

16

(Insert Table 5)

Finally, applying formula (Eq. 12), the global estimate $\hat{B}(R)$ of the glass eel biomass $B(R)$ for the 9 December 1999 and the associated approximate 95% confidence interval are:

$$\begin{cases} \hat{B}(R) = 1597\,kg, \\ IC_{95\%}(B(R)) = [1148\,kg \; ; \; 2046\,kg]. \end{cases}$$

6. DISCUSSION AND CONCLUSION

The methodology proposed is simple and needs a limited set of hypotheses: one environmental variable is important to control the migratory behaviour of fish and a sparse sampling in space and time. Information on factors that could affect the glass eel behaviour into the estuary such as turbidity, water temperature can be used to build more accurate models for the glass eel densities and sampling protocols.

A more sophisticated approach, namely via a time-space process modelization, would not be judicious due to the sparsity of the data, the great variability of the phenomenon and the lack of *a priori* knowledge hindering the use of more restrictive hypotheses.

Also, it ought to be mentioned that the variability of the water level during the flood tide has not been taken into account. This leads to some underestimation of the biomass, which is on the conservative side considering the goal of resource protection.

It is legitimate to wonder whether the modelization of the density can be improved since this is the dominant source of error. This requires more precise knowledge about the behaviour of the fish.

Values of daily glass eel biomass given here seems to be underestimated because many people think that larger glass eel are not caught in the investigation area as they migrate deeper.

Summarizing the glass eel densities near the bottom by one sampling point located far away from it should be regarded as significant underestimates.

One important point is that the sampling design is relatively simple and reproducible on others estuaries of rather large width for a low cost.

Finally, one may also wonder whether the present approach may be generalized to other fish species. The most specific aspect of this study being the relation of density to current speed, the corresponding model is certainly to be adapted to other situations. In the absence of alternative specific elements, a model with constant density with respect to time can be used. In fact, this rough approach has been tested on our data and the estimations, including confidence intervals, turned out to be rather similar. This is not so surprising since the relation of density to current speed was barely significant. It appears that the proposed methodology is strongly dependent on the experimental set up, but less though on the behavioural pattern of the fish.

With the estimates presented here, but bearing in mind all the uncertainties associated with the analysis, we may well be getting nearer to being able to estimate the fishing impact on glass eel abundance in all the estuaries. The estimated biomass of the Adour estuary is probably underestimated by the method described because the surveys do not cover the full extent of the stock into the water column and the fraction of the glass eel run possibly located close to the bottom is not taken into account. But nevertheless, biomass estimates evolution along the migratory season are compared to the evolution of professional catches showing comparable patterns. This methodology is actually used on other european sites : the Isle River and the Loire River (France), the Oria River (Spain) and the Minho River (Portugal).

ACKNOWLEDGEMENTS

REFERENCES

Anonymous (2003) Report of the International Council for Exploration of the Sea/European Inland Fishery Advisory Commission working group on Eels. ICES C.M. 2003 / ACFM: 06.

Cantrelle I. (1981) Étude de la migration et de la pêche des civelles (*Anguilla anguilla L.* 1758) dans l'estuaire de la Gironde. Ph.D. thesis, University of Paris VI.

Chen J., Thompson M.-E. and Wu C. (2004) Estimation of Fish Abundance Indices Based on Scientific Research Trawl Surveys. Biometrics, 60, 116-123.

Désaunay Y., Lecomte-Finiger R. and Guérault D. (1993) Mean age and migration patterns of *Anguilla Anguilla* (L.) glass eels from three french estuaries (Somme, Vilaine and Adour rivers). 8th session of the EIFAC working party on eel.

Hankin D.G. and Reeves G.H. (1988) Estimating total fish abundance and total habitat area in small streams based on visual estimation methods. Can. J. Fish. Aquat. Sci., 45, 834-844.

Léauté J.P. and Caill-Milly N. (2002) Synthèse halieutique et socio-économique. Technical report contract PECOSUDE European Commission/Direction Générale FISH 99/024.

Overton S. W. and McDonald T. L. (1998) Regional Estimation of Juvenile Coho Abundance in streams. West technical Report #98-5.

Prouzet P. *et al.* (2002) Historique des captures de civelles, intensité actuelle de leur exploitation, variation de leur capturabilité par la pêche professionnelle maritime et indices de colonisation sur le bassin versant de l'Adour. Technical Report, contract European Commission/Direction Générale FISH 99/023, agreement 00/1213516/NF.

Prouzet P. *et al.* (2003) Etude sur la civelle (*Anguilla anguilla* L.) dans l'estuaire de l'Adour. Pêche, biologie, comportement, modélisation hydrodynamique et comportementale, estimation des flux de civelles dans l'estuaire. Technical Report, contract Institution Adour.

Rivoirard J., Simmonds J., Foote K., Fernandes P. and Bez N. (2000) Geostatistics for Estimating Fish Abundance, Blackwell Publishing Ltd.

Rückert C., Floeter J. and Temming A. (2002) An estimate of horse mackerel biomass in the North Sea, 1991-1997. ICES Journal of Marine Science, 59, 120-130.

Schwarz C.J. and Seber G.A.F. (1999) A review of estimating animal abundance III. Statistical Science, 14, 427-445.

Thompson W. L. (2003) Hankin and Reeves' Approach to Estimating Fish Abundance in Small Streams: Limitations and Alternatives. Transactions of the American Fisheries Society, 132, 69-75.
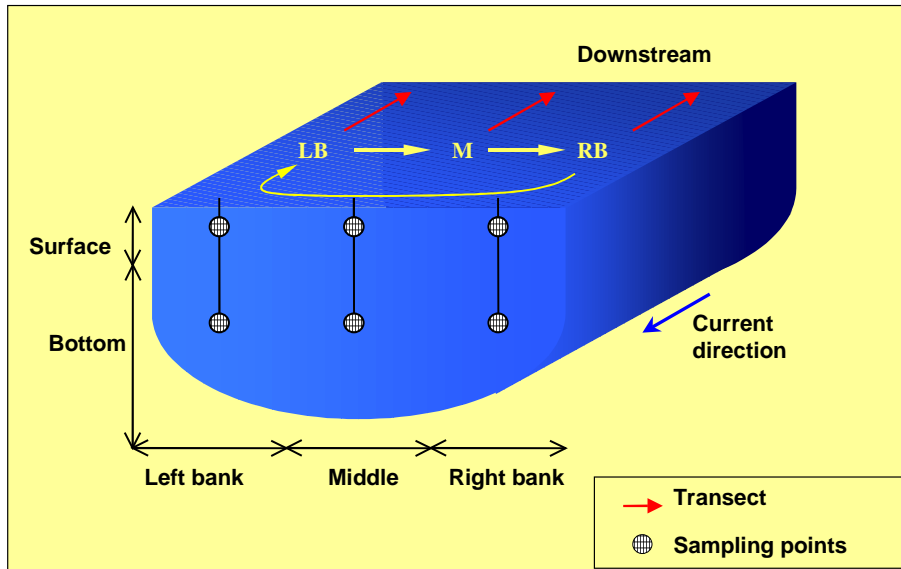
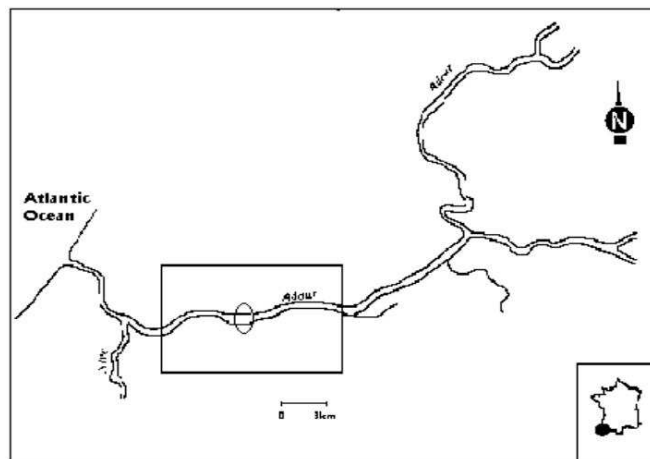**Figure 1.** Schematization of the river with sampling points.

Figure 2. The Adour estuary (43°30'N and 1°32'W) with experimental zone (ellipse) and professional fishing zone (rectangle).
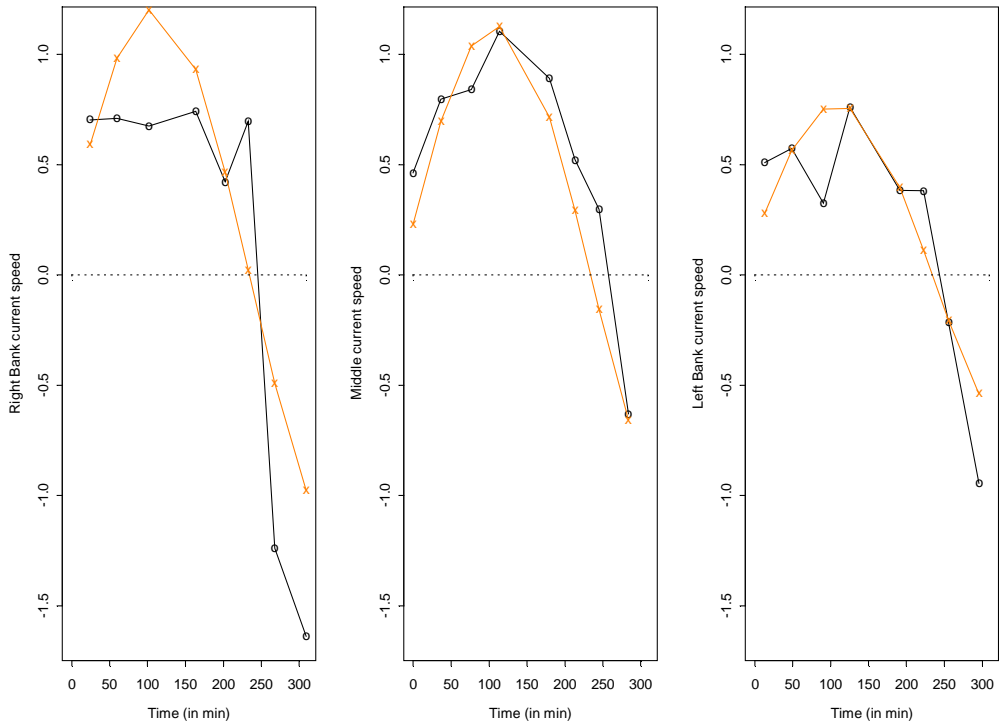
Figure 3. Current speed (in m.s^{-1}) measured *in situ* (O) compared to predicted values (×) using sinusoidal model, for

the 3 transects (RB, M, LB) for the 9 December 1999.

Figure 4. Glass eel density (g.$(100m^3)^{-1}$) in surface and depth of 4m versus current speed (modelized in m.s^{-1}) : 9
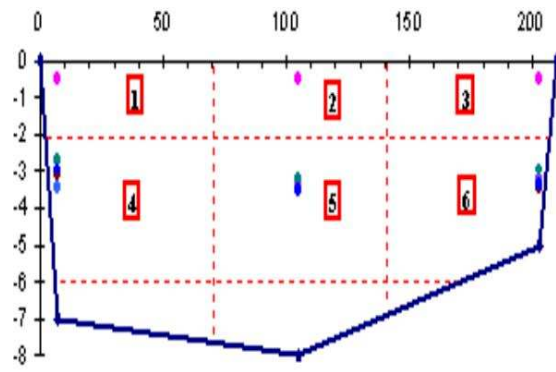
December 1999.

Figure 5. Mean section of the Adour river during the flood tide ; locations of the experimental catches (dots) and example of spatial partition (short dashes) with its associated numbering.

TABLES

TABLE 1. Parameter estimates for sinusoidal model for current speed (9 December 1999).

Parameter	Estimate	Asymptotic Std. Error
c_1	1.21	1.01
c_2	1.13	1.07
c_3	0.77	1.01
a	250.44	94.57
b	16.36	81.89

TABLE 2. Parameter estimates of density model at bottom-middle location (9 December 1999).

Parameter	Estimate	Asymptotic Std. Error
α_5	0.34	0.26
β_5	2.30	0.25

TABLE 3. Estimated biomass for one spatial scheme (9 December 1999).

Area	Description	Surface(in m^2)	$\hat{B}_s$ (in kg)	$s^2\left(\hat{B}_s\right)$
S_1	RB Surface	60	401	31566
S_2	M Surface	90	601	22243
S_3	LB Surface	60	355	20581
S_4	RB Bottom	300	1048	77365
S_5	M Bottom	450	1700	346802
S_6	LB Bottom	300	985	163105

TABLE 4. Description of the various spatial schemes.

Scheme	Widths (in m)	Depths	Implicit gradient
1	40*130*40	1*5	Edge ++ ; Surface +
2	50*110*50	1*5	Edge + ; Surface +
3	60*90*60	1*5	Center + ; Surface +
4	70*70*70	1*5	Center ++ ; Surface +
5	40*130*40	1,5*4,5	Edge ++ ; Surface = Bottom
6	50*110*50	1,5*4,5	Edge + ; Surface = Bottom
7	60*90*60	1,5*4,5	Center + ; Surface = Bottom
8	70*70*70	1,5*4,5	Center ++ ; Surface = Bottom
9	40*130*40	2*4	Edge ++ ; Bottom +
10	50*110*50	2*4	Edge + ; Bottom +

| 11 | 60*90*60 | 2*4 | Center + ; Bottom + |
| 12 | 70*70*70 | 2*4 | Center ++ ; Bottom + |

TABLE 5. Estimated biomass and standard error (in Kg) for each spatial scheme (9 December 1999).

j	1	2	3	4	5	6	7	8	9	10	11	12
$\hat{B}_j$	1620	1547	1474	1401	1523	1455	1386	1318	1426	1362	1299	1235
$s(\hat{B}_j)$	396	347	304	269	357	313	274	243	319	280	245	218